Composite Roofing of PIR Sandwich Panels: Numerical and Experimental Approach

Composite Roofing of PIR Sandwich Panels: Numerical and Experimental Approach

Mircea Georgescu [1,2], Viorel Ungureanu [1,2], Liviu Marsavina [1], Andra Floricel[1], Aurelian Gruin[3]

[1] Politehnica University, CMMC, Str. Ioan Curea, nr.1, Timisoara, Romania
[2] Romanian Academy, Timisoara Branch, CCTFA, Bd. Mihai Viteazul, nr. 24, Timisoara, Romania
[3] INCD-URBAN-INCERC, Timisoara Branch, Str. Traian Lalescu, nr. 2, Timisoara, Romania

gemircea@yahoo.com

Abstract. The PIR panels are composite elements made of an inner core of poly-iso-cyanurate (PIR) solid foam injected between two external sheets of fabric or polypropylene. When testing composite samples having such structure the obtained results (in terms of compression and bending resistances) usually reach relatively high levels. This suggests a possible use of panels in applications under distributed loading and not only as simple thermos-insulating layers. A large range of applications thus derives, i.e. cladding of timber roofing, sloping support for hydro-insulation in flat concrete roofs, or hydro-insulation support for trapezoidal sheeting for flat or even curved roofs. The paper presents an experimental and numerical study on two practical cases, i.e. flat concrete roofs and trapezoidal sheets roofs respectively. Standard testing of samples, taken from the composite core and from the membrane, have been performed in the frame of present investigation together with testing of some composite samples in compression and bending. Typical roof loading as gravity (dead + snow) load or wind suction have been analysed in the numerical simulation (reproducing the test arrangement) in order to assess panel response and to evaluate the practical applicability of these composites. Conclusions on stress distribution and deflections both under gravity and uplift load are presented. The high resistance of PIR composite panels (well beyond design loads calculated by the code) is confirmed, clearly indicating their practical applicability in the cases under study. This also meets the producer requirements who intends to obtain in the future an official agreement allowing to supply these particular composite solutions using PIR on the market.

1. Introduction - Laboratory testing

The present study is focussed on assessing the behaviour of PIR composite panels and their capability of providing a reliable support in two practical cases of frequently used roofing systems. A laboratory investigation has been performed to that purpose in order to measure the material characteristics, followed by the testing of two experimental arrangements describing the particular roof situations under study and also by subsequent numerical analysis modelling these arrangements. This has enabled the research team to drive some pertinent conclusions concerning the applicability of the panels under study in building in a new manner common type roofing with a considerable improvement of their energetic features.

The laboratory testing of PIR foam characteristics under axial compression has produced a number of results confirming the well-known pattern of stress-strain plots indicated in [1] where such foams show a plot either with hardening tendency or with a yielding tendency (yielding plateau –see fig. 1).

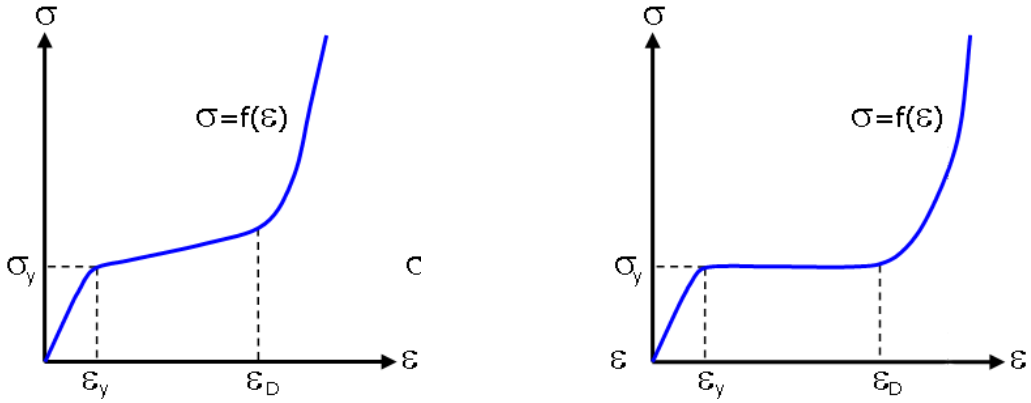

a) Hardening plateau plot b) Yielding plateau plot

Figure 1 – Specific stress-strain plots for PIR foams

As visible in fig. 1, the compression stress-strain plot may be divided in three specific zones i.e. linear elastic zone, plateau zone and densification zone. During the compression testing process a number of characteristics are usually determined i.e. the elastic modulus (E), the yield stress (σ), the plateau stress (σ_p) and the densification (ε_D). To that purpose quasi cubic samples (50x50x55mm) have been used, cut from PIR foam plates on relevant manufacturing direction and tested as per [2]. An image describing the prepared group of samples is presented in figure 2.

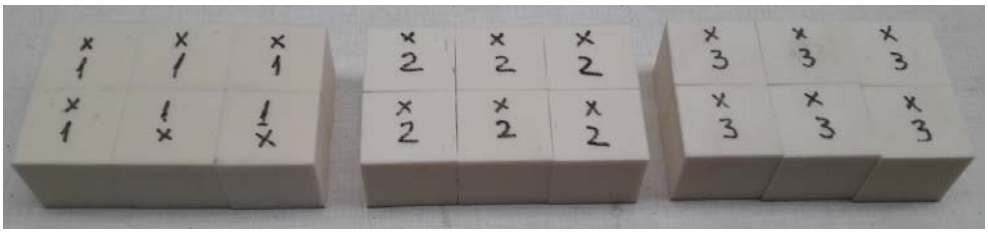

Figure 2 – PIR foam samples for compression test

Figure 3 – Testing machine for compression

Prior to the compression test the bulk density of the foam was established as per [3] using a precision balance Kern having a precision of 0,001 g and a Mytutoyo calibre with a precision of 0,1 mm resulting in a value of 35 kg/m^3. The actual testing procedure has then conducted on a Zwick Proline Z005 machine with maximum compression capacity of 5kN (see figure 3). The obtained results are presented in figure 4 (i.e. obtained stress-strain plots for all 3 directions of the foam response) and in table 1 respectively. As observed the obtained plots are very similar to the ones described in literature.

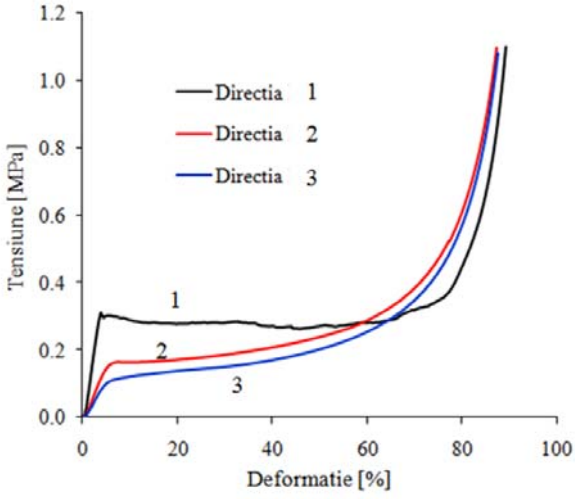

a) Stress-strain obtained plots

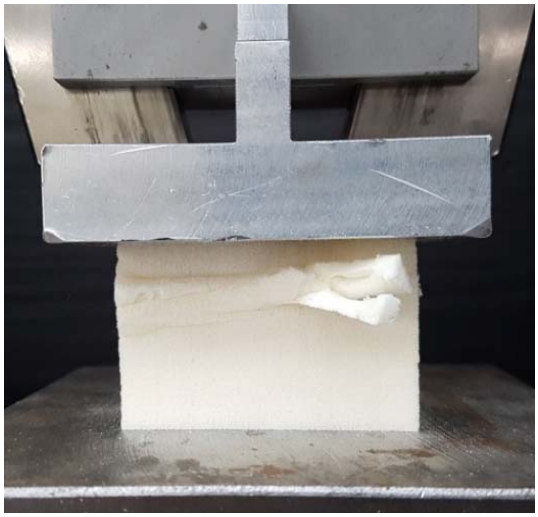

b) Foam failure for direction 1

Figure 4 – Behaviour of PIR foams under compression

Table 1. Average values of mechanical characteristics under compression

Loading direction	Sample dimensions			Elastic modulus	Yield stress	Plateau stress	Densification
	b1 [mm]	b2 [mm]	h [mm]	E [MPa]	σ_y [MPa]	σ_p [MPa]	ε_D [%]
1	54	50	50	10.42	0.32	0.28	66.14
2				3.71	0.16	0.18	60.06
3				2.88	0.12	0.15	58.81

The values of the foam characteristics presented in table 1 clearly show the anisotropic response of PIR samples with direction 1 values considerably higher than those for directions 2 and 3. Also, the yielding plateau is more extended for direction 1 plot.

For the laboratory testing of PIR foam samples under bending a number of 6 samples were used of the type described in figure 5a. These samples have been cut from a PIR plate along longitudinal and also transversal direction of foam injection and have three different lengths i.e. L=280, 330 and 380 mm respectively. Sandwich type samples thus resulted with the outer faces of 1.5 mm thick fabric sheet. The testing procedure under bending was conducted on the same testing machine as in the compression case, i.e. Zwick Proline Z005, by applying a three points scheme (see fig. 5b) with a span between supports of l=240, 280 and 320 mm respectively. The testing has been conducted at room temperature following a slow continuous pattern without shocks and with a speed of 10mm/min. The resulting force displacement plots for all spans and directions of the material are presented in figure 6 below. In all cases a linear elastic zone is visible on the plot after which an indentation appears in the contact zone

with the mid-span cylinder applying the load followed by a final rapid rupture (after failure of the membrane on the tension face).

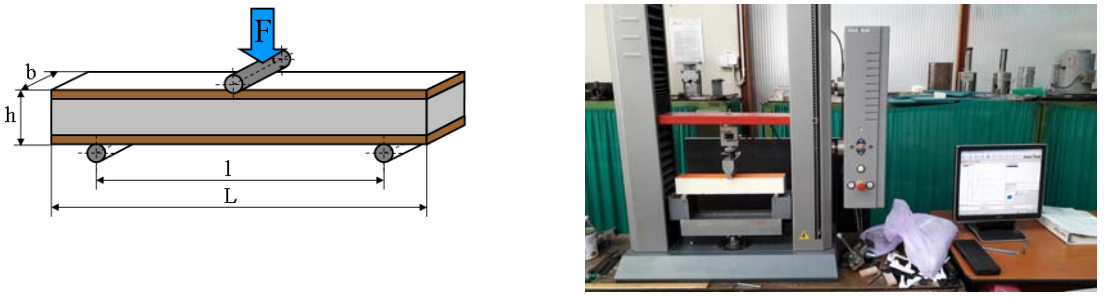

a) Sandwich type PIR sample b) Three point bending test of the sample

Figure 5 – Bending test for Thermoconfort –PIR samples

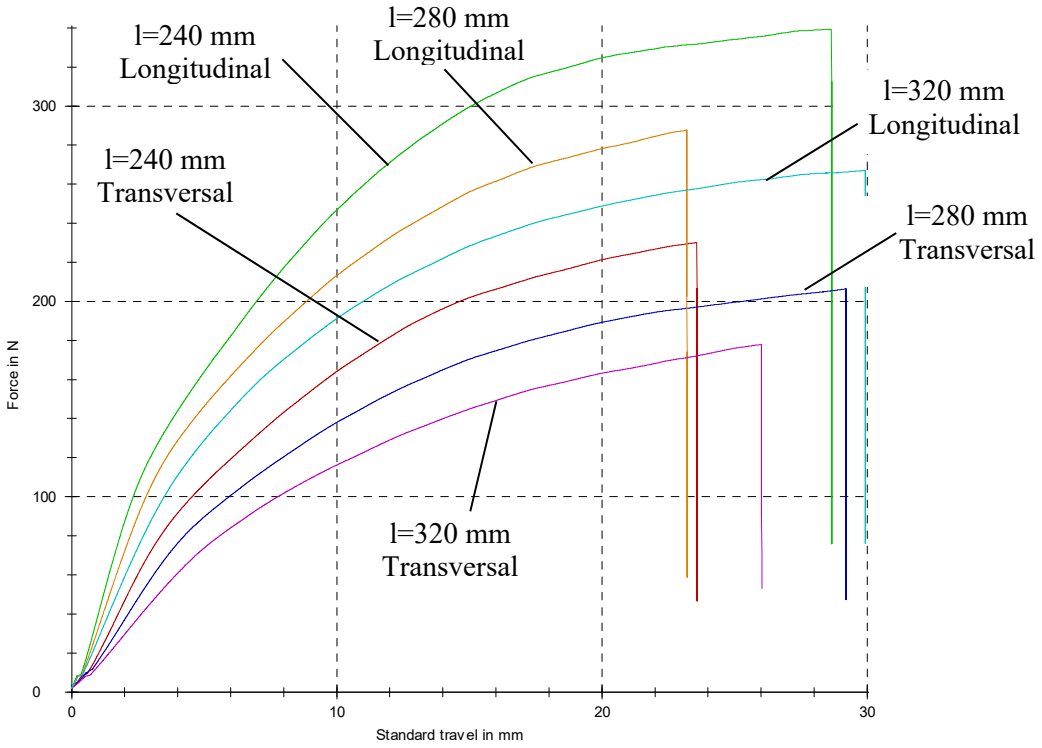

Figure 6 – Force-deflection plots by bending test

Based on maximum applied force measured via experiment, the sample bending resistance was determined using the equation below:

$$\sigma_i = \frac{3 F_{max}\, l}{2\, b\, h^2} \quad [MPa] \tag{1}$$

in which:

F_{max} =is the maximum measured experimental force in[N]
l =span between testing machine supports in [mm]
b = width of sample cross section in [mm]
h = depth of sample cross section in [mm]

The average values of results of the three points bending test considering the maximum measured experimental force F_{max} and the bending resistance σ_i are presented in table 2.

Table 2. Average values of results for the three points bending test

Span between supports l [mm]	Loading direction	Sample width b [mm]	Sample depth h [mm]	Maximum load F [N]	Bending resistance σ_i [MPa]
320	Transversal	59	59	187.6	0.44
	Longitudinal			277.8	0.65
280	Transversal			222.4	0.46
	Longitudinal			293.0	0.60
240	Transversal			243.4	0.43
	Longitudinal			329.4	0.58

For all span values under analysis the maximum loads measured and the coresponding bending resistances have been 30% larger for the longitudinal direction compared to the transversal direction. It is also visible that the bending resistance is not actually influenced by the span value between supports, beeing equal to 0.41 MPa for samples cut on transversal direction and 0.61 MPa for samples cut on longitudinal direction. The failure pattern under bending test is visible in figure 7

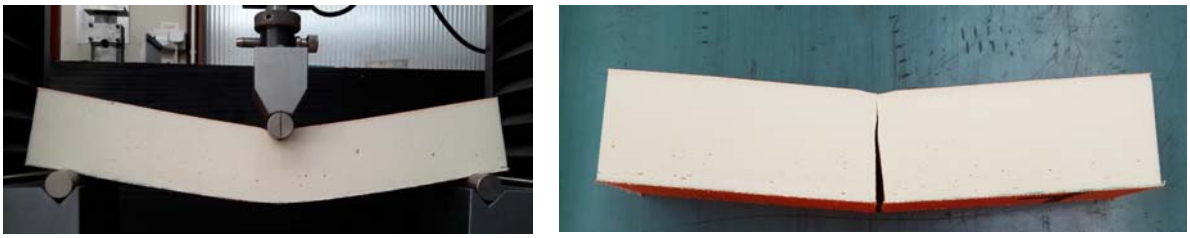

a) Indentation at upper face b) Failure of the tension face

Figure 7. Failure of the samples under bending test

As conclusions of the material testing the plastic PIR foams exhibit a high capacity of absorbing the deflection energy under compression but only fragile behaviour under tension [4], [5]. In bending, a fragile failure has been observed after prior indentation in load application zone. The obtained results for the PIR foam having a bulk density of 35 kg/m^3 clearly indicate an anisotropic behaviour with distinct properties on the three loading directions under compression respectively on transversal and longitudinal direction in bending.

2. Three-point bending test - numerical model for calibration

Following the experimental program aiming to determine the material characteristics, numerical simulations were also performed using ABAQUS 6.7 [6] in view of calibrating and validating the experimental models and also to facilitate a further parametric study. The described samples for three-point bending test have been used in simulation using bulk density value of 35 kg/m^3 for the foam core. The model has been built of three distinct layers i.e. the foam core (59x56 mm) and the outer face sheets of polypropylene 1.5 mm thickness each. The considered elasticity module was E=10.42 N/mm^2. The behaviour model for PIR Thermoconfort foam was elasto-plastic with yielding plateau and further hardening, similar to the one determined by experiment. Crushable Foam option was chosen to model

the plastic behaviour of the foam, with volumetric hardening, using a yield stress value of 0.32 N/mm^2, a plateau stress of 0.28 N/mm^2 and a densification of 66.14%. One single direction was chosen for load application i.e. direction 1. The material in the faces was modelled based on literature data [7] with a bulk density of 756.6 kg/m3 and an elasticity module E=1.0 N/mm^2. For the elastic-plastic model a yield stress value of 7.4 MPa was employed with a 8% ultimate strain.

All samples partitions created in FEM simulation have used BRICK elements type C3D8R, with 8 nodes, reduced integration and 6 DOF per nod. On the purpose to obtain accurate results, an explicit dynamic analysis was applied with displacement control. The foam core was connected to the polypropylene faces using TIE finite elements, thus trying to simulate the existing glue effect between core and faces. The model was built, analysed and controlled by comparison with similar specimens documented in literature [7], [8], [9], [10]. Two distinct types of samples have been modelled and analysed i.e. 240x59x59 mm and 320x59x59xmm respectively. The final stress distribution has resulted similar in both cases (see fig. 8) with sample failure of fragile type by rupture of the bottom face sheeting.

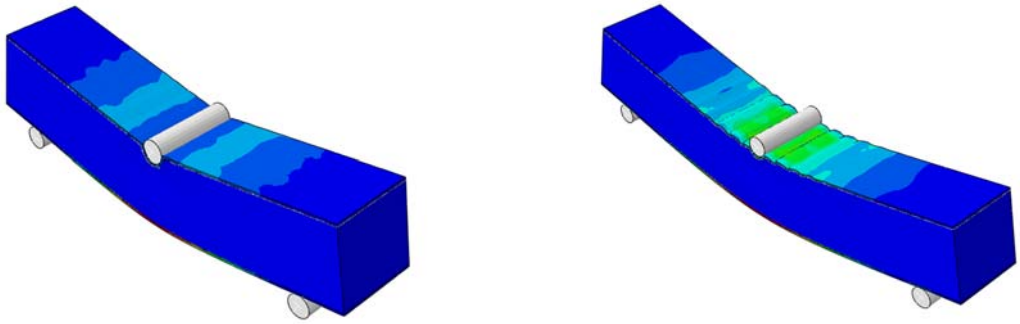

a) Sample type 240x59x59 mm Sample type 320x59x59xmm

Figure 8. Numerical models for the three-point bending test

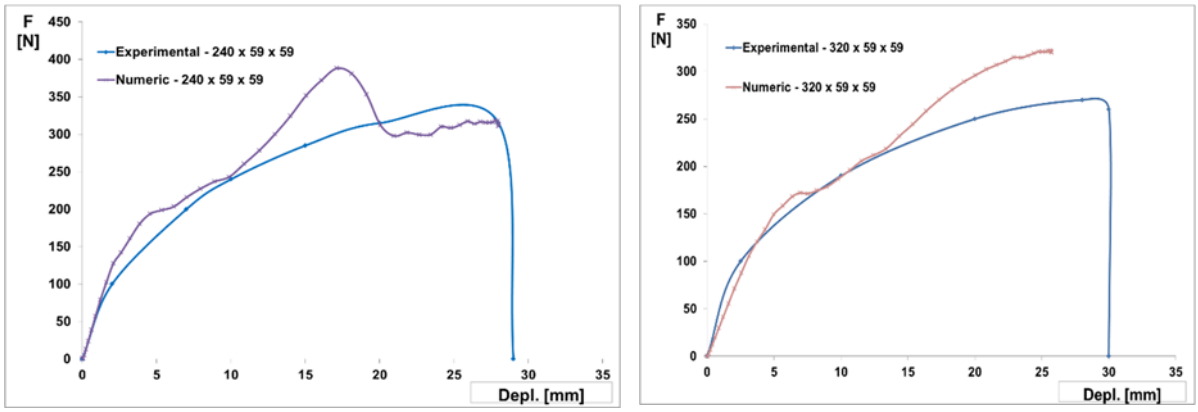

a) Sample type 240x59x59 mm b) Sample type 320x59x59 mm

Figure 9. Force displacement plots (experimental versus numerical)

In both cases the foam core undergoes a pronounced densification effect (compacting) prior to allow for the sample failure by fragile bending. For the first type of sample the observed indentation effect of the upper face sheeting was stronger owing to a higher influence of shear force while for the second type, a wrinkling pattern was observed at the level of the upper sheet (not actually obtained via experiment but possible in reality). In view of assessing the bending capacity for the foam-sheeting

composite and of calibrating the material model according to the experiment, the two force-displacement plots (experimental versus numerical) were compared in both cases under analyse (see figure 9). Similar patterns were observed for both plots in each case, as visible on the diagrams thus validating the models.

3. Full scale model using Thermoconfort panel on sloping stubs

Based on the validated material models a full scale set-up was built in the laboratory by using a Thermoconfort 6000 x 3000 x 100 mm sloping panel supported by stubs with variable height (i.e. 120, 100, 80, 60, 40, 20 mm) cut from the same material. Upper validated materials and types of finite elements were used for the foam core and panel faces. This scheme was meant to simulate the roof slope in the real case of a flat roof (very frequent in practice). Following the experimental program conducted to determine the material characteristics, numerical simulations were also performed using ABAQUS 6.7 [6] in view of calibrating and validating the experimental models and also to facilitate a further parametric study.

Both pressure and suction loads were applied (in turn) to the model. The pressure load is resulting in practice by snow action while the suction load results from wind action on the roof. As mentioned before, the foam core and the outer sheets of the panel have been interconnected in the model on the entire surface using TIE type elements and trying to simulate the glue effect between panel layers. In order to simulate the effect of mechanical fasteners connecting the roof to the sub-structure, the fastener stress plates were modelled at panel upper face as 82x40 mm rigid un-deformable rectangular elements located each 250 mm, then connected using TIE elements to the bottom face [10]. These elements had displacements and rotations blocked on all directions for the suction case and similarly for the pressure case except the displacement on the direction of the load. As for the supporting PIR / Thermoconfort stubs, these were restrained only at the base (contact zone with concrete) thus allowing for deformation / deflection of their upper zones in contact with the panel. The final numerical model for the experimental set-up is presented in figure 10

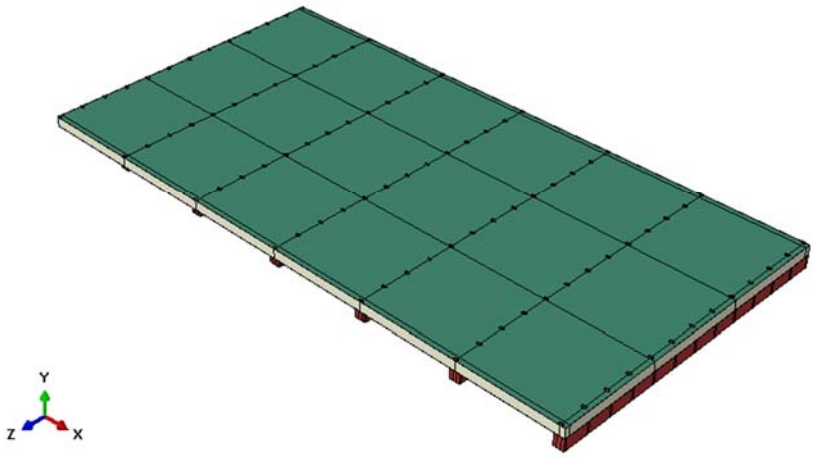

Figure 10. Numerical model for the full-scale experimental set-up supported by sloping stubs

The stress distribution obtained via FEM analysis is presented in figure 11 a) for the pressure case and in figure 11 b) for suction case respectively. Simulation as close to reality as possible of fasteners and their stress plates plays a very important role in the accurate modelling of panel response, especially under suction. The maximum stresses appear in the contact zones between foam and stress plates possibly allowing for foam rupture. Maximum deflections appear at mid-span between supports,

especially in the extreme outer spans. Nevertheless, small displacements appear in the support zones, owing to stub compression / extension. Distortion phenomena or lateral failures were observed in the stubs behaviour.

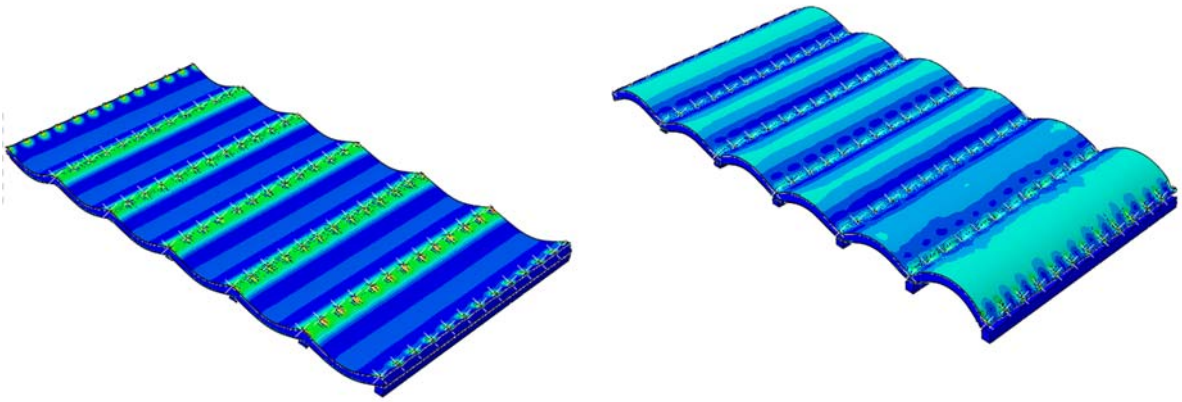

a) Panel submitted to pressure b) Panel submitted to suction

Figure 11. Stress distribution of PIR / Thermoconfort panels on sloping studs

When examining the force-deflection plots derived from FEM analysis for the two loading cases, (see figure 12) a higher resistance of the panel is observed in the pressure case while larger displacements are visible in the suction case.

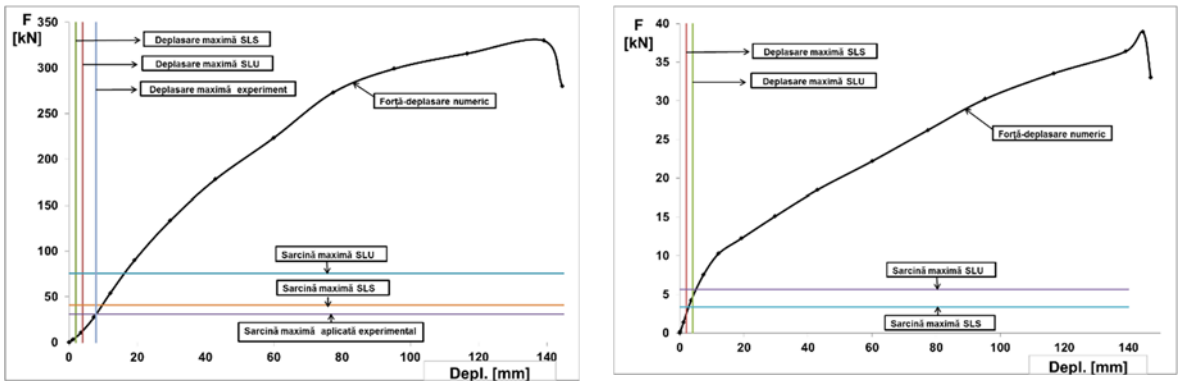

a) Pressure load b) Suction load

Figure 12. Force–deflection plots for PIR / Thermoconfort panel on sloping studs

The fact should be mentioned that both for pressure and for suction load the FEM model resistance to failure of the Thermoconfort composite panel largely exceeds the level of the design load calculated to the code as well as the experimentally applied loading (which was stopped prior to setup failure). Furthermore, the deflection value assessed on the model remains elastic within the limits of the experimental loading.

4. Full scale model using Thermoconfort panel on deep corrugation trapezoidal sheet support

A second type of experimental arrangement set up in the frame of present research was the flat roof system built of Thermoconfort / PIR panels supported by deep corrugation trapezoidal steel sheet 158 mm x 0.88 mm. Actually this is a very frequent type of flat roof applied in practice usually employing however mineral wool as thermal insulation. This stimulates the interest to replace this material with a Thermoconfort panel thus observing the response of the later to load combinations typical to such roofs. Previous FE model was thus modified to that purpose by eliminating the supporting stubs and replacing

them with trapezoidal sheeting. In order to simplify the FE model as well as for a faster convergence the number of finite elements was reduced by reducing plate width from 6000 mm to 1000 mm. Also, the presence of trapezoidal sheet in the arrangement was simulated by reducing it to its upper flange only (i.e. a system of steel plates 119 mm x 0,88 mm located at 250 mm interval as per the real geometry of the sheet) actually providing the support to the Thermoconfort panel. These flanges were modelled using SHELL type S4R elements with 4 nodes, reduced integration and 6 DOF. The employed material for the simulation was an elastic-plastic one corresponding to S350 GD steel grade. Some specific measures were taken to simulate the fastener connecting the PIR panel to the trapezoidal sheeting i.e. a SHELL-TO-SOLID coupling link with a diameter of 5 mm between the sheet and the bottom membrane and the previously mentioned rectangular pressure plates 85mm x 40 mm at the upper face of the panel. These upper plates were connected via TYE links to the upper polypropylene membrane of the panel. The loading was applied similarly to the previous model in form of a dynamic explicit analysis. The numerical model built to simulate the experimental setup is presented in figure 13.

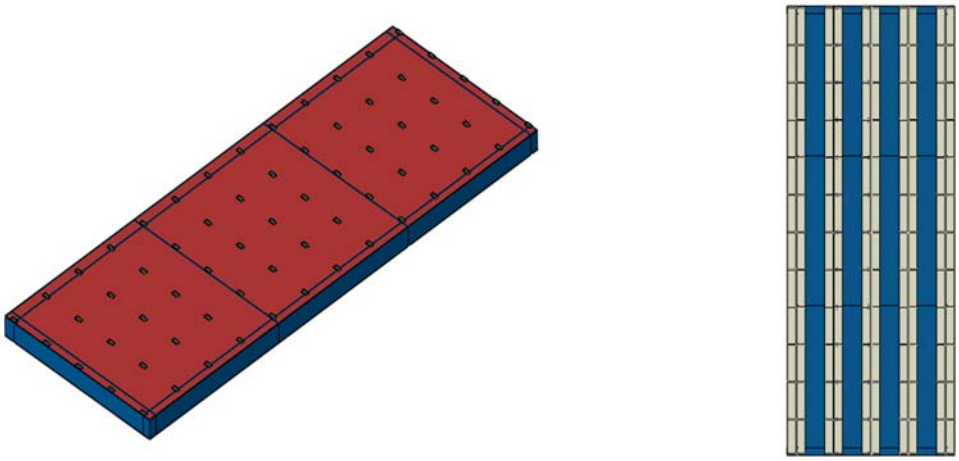

a) PIR foam panel and connections to sheeting b) Trapezoidal sheeting support

Figure 13. – Numerical model to simulate the experimental setup (testing under pressure /suction)

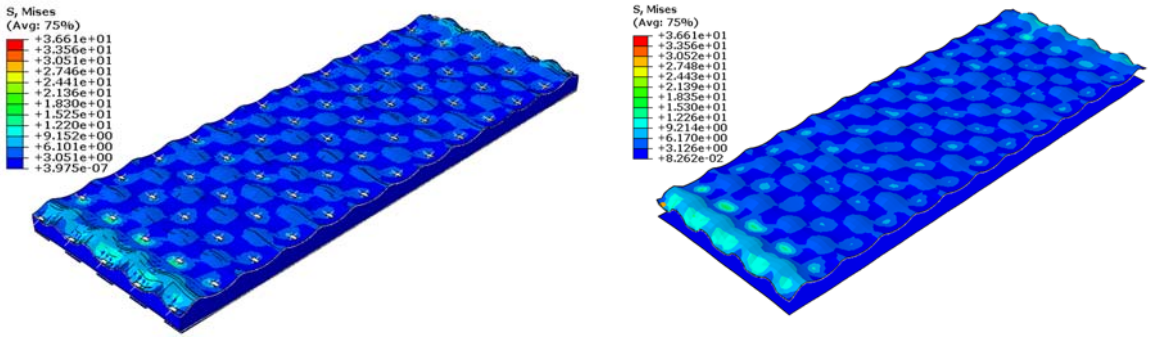

a) Stresses in the foam core b) Stresses in the membrane

Figure 14. Stress in the panel by suction modelling

The stress distribution for the model loaded with suction (more relevant for this constructional system) is presented in figure 14. Here, a simulation as accurate as possible of fasteners and of their pressure plates is playing a paramount role since the upper fibres of the foam core and the upper polypropylene membrane exhibit higher stress and deflection. This is evident especially in the zones under the pressure plate where the foam works in compression and undergoes a densification process before the fragile rupture. Both models (pressure & suction) have proved a very high resistance

considerably in excess compared to the calculated values of the ULS design load as presented in figure 15.

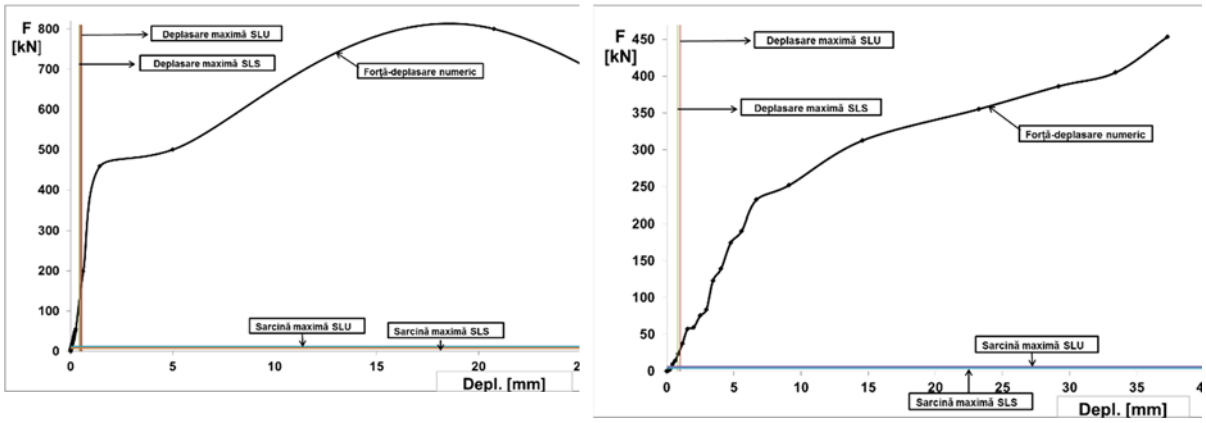

a) Pressure loading b) Suction loading

Figure 15. Force-deflection plots for the model of Thermoconfort panel on trapezoidal sheet

5. Conclusions

The experimental and numerical study performed on three distinct constructional models using composite panels (PIR foam core between two polypropylene membrane) has clearly shown a remarkable resistance of Thermoconfort, considerably in excess of the ULS calculated design loads or of the applied load via experiment. This conclusion fully satisfies customer requirement in view of practical application of such panels in projects and also of product certification by relevant authorities.

References

[1] L.J. Gibson, M. F. Ashby, "Cellular solids. Structure and properties. Second edition" *Cambridge University Press*, 1997.
[2] ASTM D 1621-00, "Standard test method for compressive properties of rigid cellular plastics"
[3] ASTM D 1622 - 03, "Test method for apparent density of rigid cellular plastics"
[4] E. Linul, "Studiul factorilor care influenteaza proprietatile mecanice ale spumelor poliuretanice rigide –Study of the factors influencing the mechanical properties of polyurethane foams", *Doctoral thesis,* Timisoara, 2011 (in Romanian).
[5] L. Marsavina, "Cellular and porous materials in structures and processes" *Edited by H. Altenbach, A. Ochsner,* Springer Verlag, 2011.
[6] ABAQUS / standard Version 6.7-1", *Int.Providence, RI: Dassault Systems*
[7] A. Boccaccio, C. Casavola, L. Lamberti, C.Pappalettere, "Structural response of polyethylene foam-based sandwich panels subjected to edgewise compression" *Materials 2013,* 6, 4545-4564; doi:10.3390/ma6104545. ISSN 1996-1944. www.mdpi.com/journal/materials.
[8] I. Ivanez, C. Santiuste, E. Barbero, S. Sanchez-Saez J. S. "Numerical modelling of foam-cored sandwich plates under high-velocity impact", *Int. J. of CEE,* Vol. 52, pp.102-117, ISSN 72 54876/x
[9] L. Hongshuai, Y. Kai, W. Weibin, Z. Hao, F. Daining "Experimental and numerical investigation on the crushing behaviour of sandwich composite under edgewise compression loading", *www.elsevier.com/locate/compositesb*.
[10] M. Kalajmasoumi, S.S.R. Koloor, A. Arefnia, I.S. Ibrahim, J. Mohd Yatim "Explicit dynamic simulation of high density polyethylene beam under flexural loading condition", *Applied Mechanics and Materials.* Vol. 229-231 (2012), pp.2150-2154, Trans Tech Publications, Switzerland, doi:10.4028/www.scientific.net/AMM.229-231.2150